



Title	Charge disproportionation with lattice distortion of $-(\text{BEDT-TTF})_2\text{RbHg}(\text{SCN})_4$ observed by $^{13}\text{C-NMR}$
Author(s)	Noda, Kazuki; Ihara, Yoshihiko; Kawamoto, Atsushi
Citation	Physical Review B, 87(8), 085105 <a href="https://doi.org/10.1103/PhysRevB.87.085105">https://doi.org/10.1103/PhysRevB.87.085105</a>
Issue Date	2013-02-15
Doc URL	<a href="http://hdl.handle.net/2115/52185">http://hdl.handle.net/2115/52185</a>
Rights	©2013 American Physical Society
Type	article
File Information	PRB87-8_085105.pdf



[Instructions for use](#)

# Charge disproportionation with lattice distortion of $\alpha$ -(BEDT-TTF)<sub>2</sub>RbHg(SCN)<sub>4</sub> observed by <sup>13</sup>C-NMR

Kazuki Noda, Yoshihiko Ihara, and Atsushi Kawamoto\*

*Department of Quantum and Condensed Matter Physics, Graduate School of Science, Hokkaido University, Kita-ku, Sapporo, Hokkaido 060-0810, Japan*

(Received 18 October 2012; revised manuscript received 10 January 2013; published 6 February 2013)

To explore the connection between  $\alpha$ -(BEDT-TTF)<sub>2</sub>I<sub>3</sub> and  $\alpha$ -(BEDT-TTF)<sub>2</sub>MHg(SCN)<sub>4</sub> ( $M = \text{K, Rb, Tl and NH}_4$ ) and to resolve the difference between band picture and charge fluctuation of  $\alpha$ -(BEDT-TTF)<sub>2</sub>MHg(SCN)<sub>4</sub>, we utilized <sup>13</sup>C-NMR to examine  $\alpha$ -(BEDT-TTF)<sub>2</sub>RbHg(SCN)<sub>4</sub> under the conditions with a large hyperfine coupling constant at each site. The temperature dependence of site susceptibility showed the development of spin disproportionation as observed in  $\alpha$ -(BEDT-TTF)<sub>2</sub>I<sub>3</sub>. We found that the linewidth of the A site only increased as temperature decreased from 200 to 100 K, a change associated with the development of lattice modulation. These findings indicate that density-wave modulation occurs during charge disproportionation instability.

DOI: [10.1103/PhysRevB.87.085105](https://doi.org/10.1103/PhysRevB.87.085105)

PACS number(s): 71.30.+h, 74.70.Kn, 76.60.-k

## I. INTRODUCTION

The (BEDT-TTF)<sub>2</sub>X salts are organic conductors consisting of alternating conducting sheets of BEDT-TTF and insulating sheets of anion.<sup>1</sup> These materials have been classified as  $\alpha$ -,  $\beta$ -,  $\kappa$ -, and  $\theta$ -types, depending on the arrangement of their BEDT-TTF molecules.<sup>2-5</sup> The physical properties of these salts, even those having the same chemical formula, (BEDT-TTF)<sub>2</sub>X, strongly depend on their molecular arrangement. For example,  $\kappa$ -type salts show antiferromagnetism or superconductivity,<sup>4,6</sup> whereas  $\theta$ -type salts show a charge-ordered (CO) state.<sup>7,8</sup> The  $\alpha$ -type salts, which have been intensively investigated during the past two decades, were recently found to be candidates for a Dirac electron system.<sup>9,10</sup>

The space group of  $\alpha$ -(BEDT-TTF)<sub>2</sub>X is  $P\bar{1}$ , with three independent molecules, A, B, and C, in a unit cell [Fig. 1(a)]. The B and C molecules are located on the inversion center, whereas the A and A' molecules are at general positions and are associated with inversion symmetry. The A and A' molecules form a columnar structure along the  $c$  or  $a$  axis, as do the B and C molecules. These two columns alternate with each other along the  $a$  or  $b$  axis.<sup>2,11</sup> The  $\alpha$ -type salts have been classified into two categories:  $\alpha$ -D<sub>2</sub>I<sub>3</sub> ( $D = \text{BEDT-TTF, BEDT-TSF, and BEDT-DTDSF}$ )<sup>2</sup> and  $\alpha$ -(BEDT-TTF)<sub>2</sub>MHg(SCN)<sub>4</sub> ( $M = \text{K, Rb, Tl and NH}_4$ ).<sup>11,12</sup> Hereafter,  $\alpha$ -(BEDT-TTF)<sub>2</sub>I<sub>3</sub> is abbreviated as  $\alpha$ -ET-I<sub>3</sub> and  $\alpha$ -(BEDT-TTF)<sub>2</sub>MHg(SCN)<sub>4</sub>,  $M = \text{Rb, K, and NH}_4$ , are abbreviated as  $\alpha$ -ET-Rb,  $\alpha$ -ET-K, and  $\alpha$ -ET-NH<sub>4</sub>. Despite intensive investigation of  $\alpha$ -ET-I<sub>3</sub>, the mechanism underlying the metal-insulator (MI) transition around 135 K at ambient pressure remained unclear. Investigations concluded that the insulator phase is a CO state, where the charges on the A, B, and C molecules are disproportionate to the breaking of inversion symmetry, due to off-site Coulomb interactions.<sup>13-16</sup> Moreover, the MI transition could be suppressed by pressure, and the band dispersion of the paramagnetic state is thought to have a narrow gap structure. This unconventional band structure may be a candidate for a Dirac electron system.<sup>9,10</sup>

In contrast, the physical properties of  $\alpha$ -(BEDT-TTF)<sub>2</sub>MHg(SCN)<sub>4</sub> salts are due to the density-wave (DW) state of their one-dimensional Fermi surfaces.<sup>17-21</sup>

However, the  $\alpha$ -ET-NH<sub>4</sub> salt showed superconductivity at about 1 K,<sup>22</sup> suggesting that superconductivity is mediated by charge fluctuation.<sup>23</sup> Although the incommensurate satellite reflection observed by x-ray diffraction (XRD) was consistent with the charge density wave (CDW) instability, some inconsistencies have been observed with a conventional CDW framework, including high order harmonics, marked sample dependence, and short coherence length in the DW state. Moreover, the satellite reflection was observed over a wide temperature range.<sup>20,21</sup>

Although  $\alpha$ -ET-I<sub>3</sub> and  $\alpha$ -(BEDT-TTF)<sub>2</sub>MHg(SCN)<sub>4</sub> have the same molecular arrangement, with each having a diamagnetic anion, the electronic structure of the former has been correlated with the distribution of electrons, whereas the structure of the latter was understood within the band framework. The electronic configuration of the paramagnetic phase of  $\alpha$ -(BEDT-TTF)<sub>2</sub>MHg(SCN)<sub>4</sub> thus remains unclear, although this phase involves information on the mechanism of superconductivity of  $\alpha$ -ET-NH<sub>4</sub>, which appears after the suppression of DW.

Analyses of the infrared reflection spectra of  $\alpha$ -ET-K and  $\alpha$ -ET-Rb salts suggest that the charge fluctuations are observed below 200 K.<sup>24</sup> The infrared spectrum of the  $\alpha$ -ET-K salt below 20 K clearly and independently showed breakage of inversion symmetry, suggesting that breaking of inversion symmetry occurs at low temperatures.<sup>25</sup> <sup>13</sup>C-NMR peak splitting was also observed for the  $\alpha$ -ET-Rb salt below  $T_{\text{DW}}$ .<sup>26</sup> These results and our hypothesis, that superconductivity is mediated by CO fluctuations, suggested CO instability in  $\alpha$ -(BEDT-TTF)<sub>2</sub>MHg(SCN)<sub>4</sub>.

In  $\alpha$ -(BEDT-TTF)<sub>2</sub>MHg(SCN)<sub>4</sub>, the  $a$ -axial interaction is stronger than the  $c$ -axial interaction and the one-dimensional Fermi surface perpendicular to the  $a$  axis. Therefore, the system becomes more one dimensional under the  $a$ -axial strain, and the system becomes more two dimensional under the  $c$ -axial strain. Namely, the ratio of the in-plane lattice constant,  $c/a$ , can control the dimensionality of the electronic state in  $\alpha$ -(BEDT-TTF)<sub>2</sub>MHg(SCN)<sub>4</sub>. The phase diagram of  $\alpha$ -(BEDT-TTF)<sub>2</sub>MHg(SCN)<sub>4</sub> taking the value of  $c/a$  as a tuning parameter was suggested from the uniaxial strain

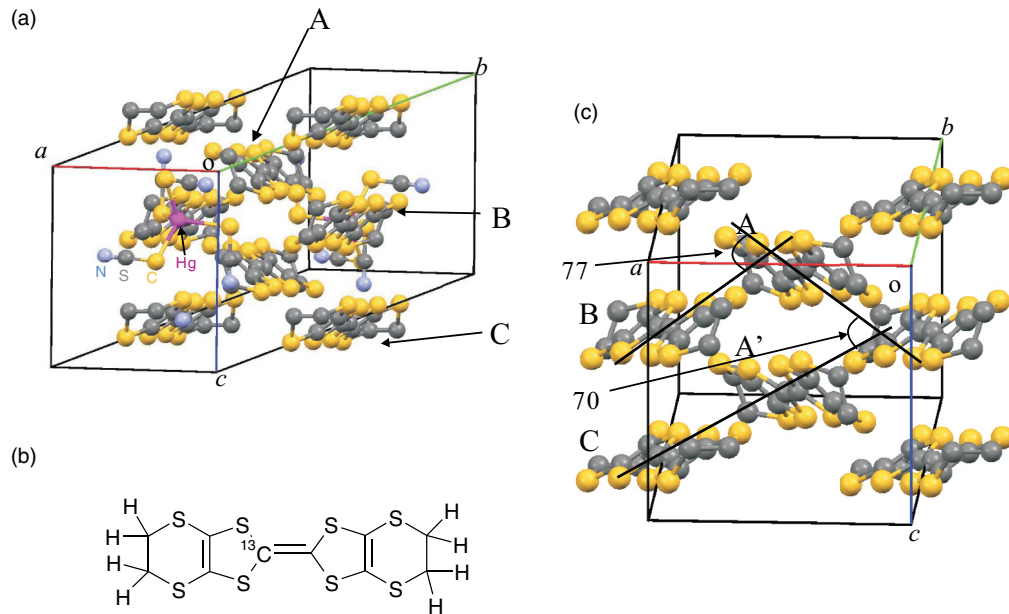


FIG. 1. (Color online) (a) Crystal structure of  $\alpha$ -(BEDT-TTF) $_2$ MHg(SCN) $_4$  (Ref. 11). (b) Molecular structure of BEDT-TTF- $^{13}\text{C}$  enriched on one side with  $^{13}\text{C}$  nuclei to prevent the Pake doublet effect. (c) Composite diagram of  $\alpha$ -(BEDT-TTF) $_2$ MHg(SCN) $_4$  viewed along the  $b^*$  axis (Ref. 11). The B and C molecules are located on the inversion center, whereas the A and A' molecules are at general positions and are associated with inversion symmetry.

experiment, as shown in Fig. 2.<sup>27</sup> Moreover, it was speculated that  $\alpha$ -ET-I $_3$  locates at the small value of  $c/a$  on the phase diagram<sup>28</sup> because the value of  $c/a$  for  $\alpha$ -ET-I $_3$  at ambient pressure is smaller than that for  $\alpha$ -ET-NH $_4$ ,<sup>2,11</sup> and  $\alpha$ -ET-I $_3$  showed a SC transition under the uniaxial strain which increases the value of  $c/a$ .<sup>29</sup>

To date, no experimental evidence connects the DW observed by XRD<sup>20,21</sup> and the CO instability observed at low temperature.<sup>21,25,26</sup> Moreover, it is important to verify whether the lattice distortion in the paramagnetic state actually affects the electronic properties. Since the contribution of the off-site Coulomb interaction should be observed in the A and A' molecules, a site-selective magnetic probe is desired. Field

direction specified  $^{13}\text{C}$ -NMR is suitable for this purpose.<sup>16,26</sup> In our previous report, we performed  $^{13}\text{C}$ -NMR at the direction which we could measure in detail about the B and C molecules.<sup>26</sup> Therefore to assess the connection between DW instability and off-site Coulomb interactions, we assessed the  $^{13}\text{C}$ -NMR spectrum of this salt at the specific magnetic field direction, allowing the magnetism of the A molecule to be sensitively detected, and we compared these results with those at an angle of high sensitivity for the B and C molecules.

## II. EXPERIMENTAL DETAILS

To prevent the Pake doublet effect, we enriched one side of the central double-bonded carbon site with  $^{13}\text{C}$  nuclei [Fig. 1(b)].<sup>30</sup> Single crystals of  $\alpha$ -ET-Rb were prepared by the electrochemical oxidation method.<sup>11</sup> The crystals of this molecule typically have a black thick rectangular shape. NMR spectra were measured using a spin-echo method, with an external magnetic field of 9.4 T. The angle dependence of the NMR shift around the  $b^*$  axis was measured using the angle rotating equipment. The linewidths were measured as full widths at half maximum (FWHM) of Lorentz fitting.

## III. RESULTS AND DISCUSSIONS

### A. Site assignment and hyperfine coupling constant

Although spin susceptibility provides important information about the electronic properties,  $\alpha$ -ET-K,  $\alpha$ -ET-Rb, and  $\alpha$ -ET-NH $_4$  salts contain a number of molecules in a unit cell, with the spin susceptibility at each site behaving independently. NMR, a microscopic magnetometer, can assess the local susceptibility around the nuclei. The carbon sites of the central C=C bond on the A molecule are not crystallographically

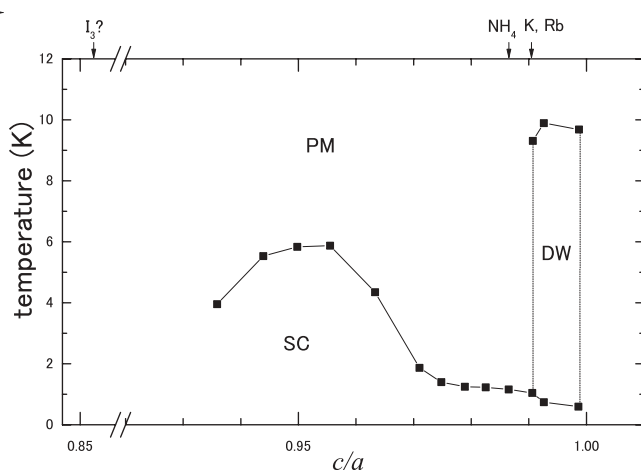


FIG. 2. Phase diagram of  $\alpha$ -(BEDT-TTF) $_2$ X determined by resistance measurement under the uniaxial strain. The horizontal axis is  $c/a$ , the ratio of the in-plane lattice constant (Refs. 27 and 28).

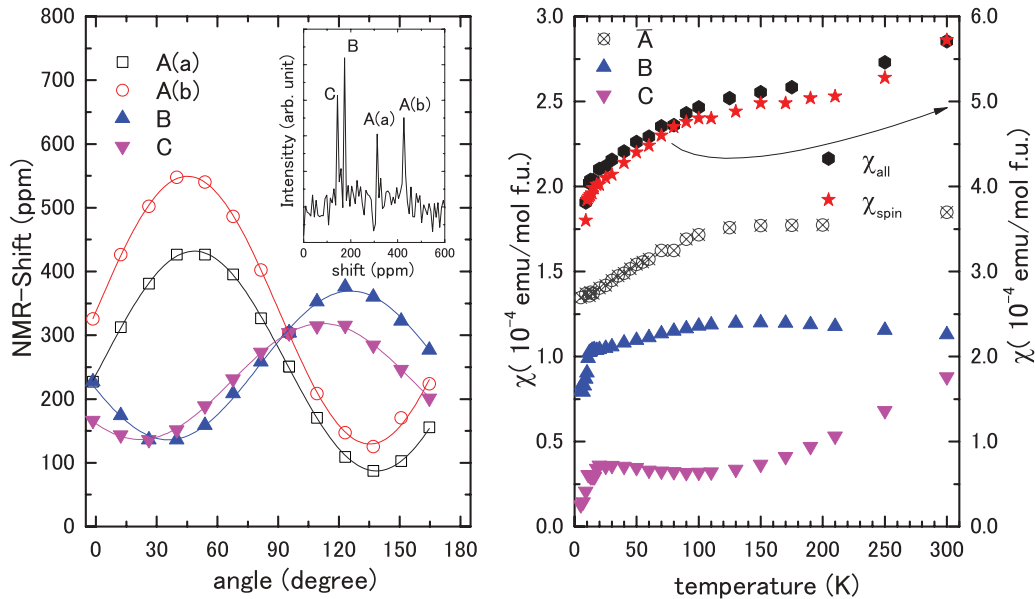


FIG. 3. (Color online) (a) Angular dependence of the NMR shift of  $\alpha$ -ET-Rb at room temperature. (Inset: NMR spectrum at  $\theta = 12.3^\circ$ .) (b) Temperature dependence of the local susceptibility of  $\alpha$ -ET-Rb deduced from the Knight shift and the spin susceptibility. [ $\bar{A}$  is the mean value deduced from the A(a) and A(b) sites.]

equivalent, whereas the sites on the B and C molecules are equivalent. Therefore, NMR spectra should show four peaks, corresponding to the independent  $^{13}\text{C}$  sites of A(a), A(b), B, and C. Indeed, we observed four peaks at room temperature [Fig. 3(a), inset]. These peaks could be assigned to their corresponding molecules by the phase of the NMR shift during measurement of angle rotation. Figure 3(a) shows the angular dependence of the NMR shift around the  $b^*$  axis. The anisotropic shift is mainly dependent on the dipole field of the electronic spin in the  $p_z$  orbital. When the field is parallel to the  $p_z$  orbital, the NMR shift reaches a maximum, whereas when the external magnetic field is perpendicular to the  $p_z$  orbital, the NMR shift reaches a minimum. As the A(a) and A(b) sites are on the same molecule, and the  $p_z$  direction of the two sites are parallel to each other, the angular dependencies of the A(a) and A(b) sites should be in the same phase. Therefore the open circle and square symbols in Fig. 3(a) could be assigned to the signals from the A(a) and A(b) sites, respectively. We evaluated that the angle between the A and B molecules is  $77^\circ$ , whereas the angle between the A and C molecules is  $70^\circ$  [Fig. 1(c)].<sup>11</sup> When we compared these angles with the phase difference of the angular dependent NMR shift, we found that the solid and inverted solid triangles could be assigned to the signals from the B and C sites, respectively. Using the peak assignment for the four peaks, we could evaluate site susceptibility.

The NMR shift ( $\delta$ ) can be determined from the Knight shift ( $K$ ), the chemical shift ( $\sigma$ ), and the spin susceptibility ( $\chi_s$ ), using the equation  $\delta(\theta) = K(\theta) + \sigma(\theta) = A(\theta)\chi_s + \sigma(\theta)$ . Here,  $A$  is a hyperfine coupling constant between the nuclear and electron spins. The chemical shift could be estimated from the chemical shift tensor for  $(\text{BEDT-TTF})^{+0.5}$ .<sup>16</sup> As the spin susceptibility  $\chi_s$  is isotropic, the anisotropy of the NMR shift is dependent on the anisotropy of the hyperfine

coupling constant, which is derived from the  $p_z$  orbital and does not show significant site dependence.<sup>15</sup> Therefore the ratio of local susceptibility at room temperature could be estimated from the amplitude of the angle dependent Knight shift, and the local susceptibilities could be estimated from the observed amplitudes. Thus,  $\chi_s = 2\chi_A + \chi_B + \chi_C$  as  $\chi_A(\text{RT}) = 1.9 \times 10^{-4}$  emu/mol.,  $\chi_B(\text{RT}) = 1.1 \times 10^{-4}$  emu/mol., and  $\chi_C(\text{RT}) = 0.9 \times 10^{-4}$  emu/mol.

To reliably determine the temperature dependence of local spin susceptibility, it is necessary to measure the Knight shift under conditions with a large hyperfine coupling constant. Hence, the field direction  $\theta$  of  $52^\circ$  in Fig. 3(a) is suitable to A sites with hyperfine coupling constants of  $A_{A(a)} = 11$  kOe/ $\mu_B$  and  $A_{A(b)} = 15$  kOe/ $\mu_B$ , and the field direction of  $127^\circ$  is suitable for the B and C sites with  $A_B = 17$  kOe/ $\mu_B$  and  $A_C = 11$  kOe/ $\mu_B$ .

### B. Temperature dependence of the local susceptibility

The temperature dependence of the local susceptibility estimated from the NMR shifts at the corresponding angles is shown in Fig. 3(b). The data for  $\theta = 127^\circ$  were from our previous report.<sup>26</sup> The total value ( $\chi_{\text{all}} = 2\chi_A + \chi_B + \chi_C$ ) and the spin susceptibility from SQUID measurements are also plotted in Fig. 3(b).<sup>18</sup> The temperature dependence of  $\chi_{\text{all}}$  is consistent with that of the spin susceptibility. At room temperature, the local spin susceptibilities of the B and C sites are almost the same. With decreasing temperature, however, spin disproportionation developed between the spin-rich B and the spin-poor C molecules with the order of the spin susceptibility being  $\chi_A > \chi_B > \chi_C$ .

The same spin disproportionation in the paramagnetic phase is observed above 135 K for  $\alpha$ -ET-I<sub>3</sub>.<sup>16</sup> In both salts, the molecule forming with the larger dihedral angle the A

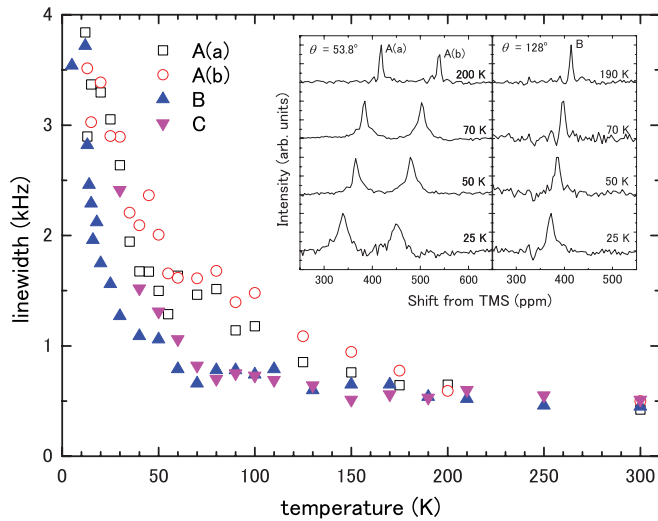


FIG. 4. (Color online) Temperature dependence of the linewidth of NMR shift of  $\alpha$ -ET-Rb. (Inset: NMR spectra for the A(a), A(b), and B sites)

molecule became the spin poor site. Spin susceptibility can be determined by the density of state at Fermi energy, and is almost temperature independent in the band regime. Hence the temperature dependent disproportionation is regarded as due to the electron correlation. Since  $\alpha$ -ET- $I_3$  undergoes CO transition, the similarity of the spin disproportionation including the temperature dependence for the  $\alpha$ -ET-Rb and  $\alpha$ -ET- $I_3$  salts suggested a CO instability in  $\alpha$ -(BEDT-TTF) $_2$ MHg(SCN) $_4$  and in the unified diagram for the  $\alpha$ -(BEDT-TTF) $_2$ X system.

### C. Linewidth anomaly

However, there was definitive evidence of structural distortion, and transport measurements under high field were connected to the DW instability.<sup>19–21</sup> We explored anomalies of the  $^{13}\text{C}$ -NMR spectra associated with these structural distortions. Figure 4 shows the temperature dependence of the linewidth of the NMR shifts of the A(a), A(b), B, and C sites; the behavior of the C site at low temperature could not be evaluated due to the overlap of the C site with the A sites at these temperatures. The linewidth of the B and C sites increased rapidly from 50 to 8 K, at which  $\alpha$ -ET-Rb shows the DW transition. In contrast, the linewidth of the A site gradually increased as temperature decreased from 200 K, leveling off at around 100 K, but increased as the temperature decreased below 50 K, similar to the B site. Below 50 K, the linewidth of all sites broadened, reflecting the DW anomaly as well as the satellite reflection intensity.<sup>20,21</sup> The behavior of the A site below 200 K is reminiscent of the thermal variations of the correlation length of the satellite reflection observed on XRD.<sup>20,21</sup>

### D. Symmetry breaking at A sites

In Fourier transform (FT)-NMR, the linewidth is described as  $\Delta\omega = 2\pi/T_2 + \gamma\Delta H$ . Therefore, we could specify the static or dynamic cause of increasing linewidth through the measurement of the spin-spin relaxation time  $T_2$ . We could measure the  $T_2$  of the A(a) site, 1.03 ms (RT), 1.27 ms (50 K), and 0.99 ms (25 K). We could measure the  $T_2$  of the

A(b) site, 1.09 ms (RT), 1.17 ms (50 K), and 0.98 ms (25 K).  $T_2$  barely depends on temperature, and the linewidth due to  $T_2^{-1}$  is about 1 kHz. Hence the linewidth below 100 K is caused by inhomogeneous static width. In x-ray measurement, P. Foury-Leylekian *et al.* speculate that the super lattice of  $\alpha$ -ET-Rb and  $\alpha$ -ET-K does not couple with a fluctuation CDW of a simple electron system but with weakening symmetry of lattice. In measurement of  $T_2$  by NMR, the increasing linewidth suggests static strain, consistent with their speculation.

The differences in temperature associated behavior at the A, B and C sites provide important information about lattice distortion and electronic properties at these sites. XRD results suggested that the superlattice of  $\alpha$ -ET-K was not coupled with CDW fluctuations in a normal manner but with static anion distortion combined with the CDW instability.<sup>20,21</sup> It is therefore unclear whether the broadening is due merely to the lattice distortion or involves electronic anomalies. Static lattice modulations can broaden NMR linewidth. For example, potential disorder due to a structural modulation can induce electron localization and change the distribution of local susceptibility.<sup>31,32</sup> This distribution can broaden the linewidth through the hyperfine coupling constant ( $\Delta\delta = A\Delta\chi$ ). Alternatively, a structural modulation can modify both the molecular arrangement and the hyperfine coupling constant, resulting in broadening of the linewidth ( $\Delta\delta = \Delta A \cdot \chi$ ). Regardless, anomalous linewidths should be observed at the A, B, and C sites. However, anomalous linewidths similar to lattice modulation were observed only at the A sites.

The NMR spectrum of the A(a,b) sites in  $\alpha$ -ET- $I_3$  is split into two spectra, of the A(a,b) and A'(a,b) sites, in the CO phase. As in  $\alpha$ -ET- $I_3$ , this linewidth broadening suggests that the charge disproportionation between A and A' molecules is due to the Coulomb repulsion. The incommensurate lattice modulation distributes the amplitude of the charge disproportionation, such that the splitting should be observed as linewidth broadening. Geometrically a one-dimensional band is formed along the  $a$  axis, resulting in a disproportionation between A and A' molecules nearly perpendicular to the DW modulation.

Intercolumn disproportionation is observed at typical temperatures (Fig. 5). From room temperature to approximately

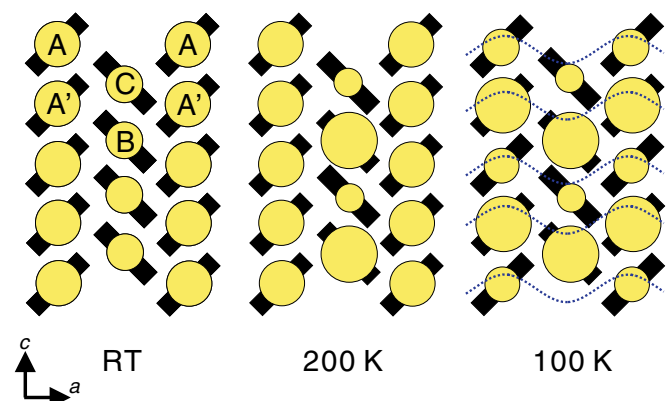


FIG. 5. (Color online) Schematic diagram of the charge disproportionation at typical temperatures. At 100 K, the DW instability was enhanced along the  $a$  axis.

200 K, the disproportionation in the BC column is enhanced, and crystallographic symmetry is unchanged. From 200 to 100 K, the disproportionation in the A column perpendicular to DW modulation emerges, suggesting the breaking of symmetry.

The estimated spin disproportionation  $\Delta\chi/\chi$  was about 0.04. Vibrational spectroscopy suggested that the degree of charge disproportionation was much smaller than that in  $\alpha$ -ET-I<sub>3</sub>.<sup>25</sup> This finding is consistent with the small disproportionation estimated from the linewidth. The charge fluctuation around 100 K is suggested by the reflection spectrum of  $\alpha$ -ET-K, which may detect the response of the disproportionate state between A and A' molecules along the *c* axis.<sup>33</sup>

Our results suggest that the paramagnetic phase of  $\alpha$ -(BEDT-TTF)<sub>2</sub>X showed CO instability, whereas, at low temperature, these phenomena differ for the CO state of  $\alpha$ -ET-I<sub>3</sub> and the DW state of  $\alpha$ -ET-Rb, a difference that may be explained by the topology of Fermi surfaces. The molecule  $\alpha$ -ET-Rb has a one-dimensional open Fermi surface, which can nest easily,<sup>11</sup> whereas  $\alpha$ -ET-I<sub>3</sub> has a characteristic band structure similar to a Dirac electron system.<sup>10</sup> The unified phase diagram of  $\alpha$ -(BEDT-TTF)<sub>2</sub>X may be described by the competition between and combination of the band shape and the CO (symmetry breaking) instability.

We note that  $\alpha$ -ET-NH<sub>4</sub> showed superconductivity when the DW transition at low temperature was suppressed. The pairing mechanism in  $\alpha$ -ET-NH<sub>4</sub> may be assessed by verifying the CO instability coupling with a DW fluctuation in the paramagnetic state. Although vibrational spectroscopy showed no anomaly in  $\alpha$ -ET-NH<sub>4</sub>, it showed an anomaly in  $\alpha$ -ET-K only below

20 K and could not detect this behavior at around 100 K.<sup>25</sup> Hence the <sup>13</sup>C-NMR spectrum of  $\alpha$ -ET-NH<sub>4</sub> is necessary.

#### IV. CONCLUDING REMARKS

In conclusion, we performed <sup>13</sup>C-NMR measurements of  $\alpha$ -ET-Rb in the direction of the large hyperfine coupling constant of the A(a) and A(b) sites. By combining the Knight shifts of the A(a) and A(b) sites and the results of the B and C sites, we found that the spin susceptibility of  $\alpha$ -ET-Rb showed spin disproportionation, similar to that of  $\alpha$ -ET-I<sub>3</sub>, which undergoes a CO transition. We found that the temperature dependence of the linewidth of the NMR spectrum at the A sites gradually increased as temperature decreased from 200 K, whereas the linewidth of the B and C sites increased rapidly from 50 to 8 K. The anomaly of A site is reminiscent of the lattice modulation observed by XRD. Differences in broadening behavior at the A and other sites could be explained by the breakage of electronic symmetry at the A sites, suggesting CO instability with DW modulation.

#### ACKNOWLEDGMENTS

The authors thank K. Yakushi of the Toyota Physical and Chemical Research Institute for valuable discussions, and T. Inabe of Hokkaido University for the determination of crystal orientation. This work was partially supported by a Grant-in-Aid for Science Research (Grant No. 24540353) from the Ministry of Education, Culture, Sports, Science and Technology of Japan.

\*atkawa@phys.sci.hokudai.ac.jp

<sup>1</sup>T. Ishiguro, K. Yamaji, and G. Saito, *Organic Superconductors*, Vol. 88, 2nd ed. (Springer, New York, 1998).

<sup>2</sup>K. Bender, I. Henning, D. Schweitzer, K. Dietz, H. Endres, and H. J. Keller, *Mol. Cryst. Liq. Cryst.* **108**, 359 (1984).

<sup>3</sup>V. F. Kaminskii, T. G. Prokhorova, R. P. Shibaeva, and É. B. Yagubskii, *JETP Lett.* **39**, 17 (1983).

<sup>4</sup>H. Urayama, H. Yamochi, G. Saito, K. Nozawa, T. Sugano, M. Kinoshita, S. Sato, K. Oshima, A. Kawamoto, and J. Tanaka, *Chem. Lett.* **17**, 55 (1988).

<sup>5</sup>H. Mori, S. Tanaka, T. Mori, A. Kobayashi, and H. Kobayashi, *Bull. Chem. Soc. Jpn.* **71**, 797 (1998).

<sup>6</sup>K. Miyagawa, A. Kawamoto, Y. Nakazawa, and K. Kanoda, *Phys. Rev. Lett.* **75**, 1174 (1995).

<sup>7</sup>K. Miyagawa, A. Kawamoto, and K. Kanoda, *Phys. Rev. B* **62**, R7679 (2000).

<sup>8</sup>K. Yamamoto, K. Yakushi, K. Miyagawa, K. Kanoda, and A. Kawamoto, *Phys. Rev. B* **65**, 085110 (2002).

<sup>9</sup>N. Tajima, M. Tamura, Y. Nishino, K. Kajita, and Y. Iye, *J. Phys. Soc. Jpn.* **69**, 543 (1999).

<sup>10</sup>S. Katayama, A. Kobayashi, and Y. Suzumura, *J. Phys. Soc. Jpn.* **75**, 054705 (2006).

<sup>11</sup>H. Mori, S. Tanaka, M. Oshima, G. Saito, T. Mori, Y. Maruyama, and H. Inokuchi, *Bull. Chem. Soc. Jpn.* **63**, 2183 (1990).

<sup>12</sup>R. Rousseau, M.-L. Doublet, E. Canadell, R. P. Shibaeva, S. S. Khasanov, L. P. Rozenberg, N. D. Kushch, and E. B. Yagubskii, *J. Phys. I (France)* **6**, 1527 (1996).

<sup>13</sup>H. Seo and H. Fukuyama, *J. Phys. Soc. Jpn.* **66**, 1249 (1997).

<sup>14</sup>R. Wojciechowski, K. Yamamoto, K. Yakushi, M. Inokuchi, and A. Kawamoto, *Phys. Rev. B* **67**, 224105 (2003).

<sup>15</sup>Y. Takano, K. Hiraki, H. M. Yamamoto, T. Nakamura, and T. Takahashi, *J. Phys. Chem. Solids* **62**, 393 (2001).

<sup>16</sup>T. Kawai and A. Kawamoto, *J. Phys. Soc. Jpn.* **78**, 074711 (2009).

<sup>17</sup>T. Sasaki, H. Sato, and N. Toyota, *Synth. Met.* **41-43**, 2211 (1991).

<sup>18</sup>K. Miyagawa, A. Kawamoto, and K. Kanoda, *Phys. Rev. B* **56**, R8487 (1997).

<sup>19</sup>N. Harrison, L. Balicas, J. S. Brooks, and M. Tokumoto, *Phys. Rev. B* **62**, 14212 (2000).

<sup>20</sup>P. Foury-Leylekian, S. Ravy, J.-P. Pouget, and H. Müller, *Synth. Met.* **137**, 1271 (2003).

<sup>21</sup>P. Foury-Leylekian, J.-P. Puget, Y.-J. Lee, R. M. Nieminen, P. Ordejón, and E. Canadell, *Phys. Rev. B* **82**, 134116 (2010).

<sup>22</sup>H. H. Wang, K. D. Carlson, U. Geiser, W. K. Kwok, M. D. Vashon, J. E. Thompson, N. F. Larsen, G. D. McCabe, R. S. Hulscher, and J. M. Williams, *Physica C* **166**, 57 (1990).

<sup>23</sup>J. Merino and R. H. McKenzie, *Phys. Rev. Lett.* **87**, 237002 (2001).

<sup>24</sup>M. Dressel, N. Drichko, J. Schlueter, and J. Merino, *Phys. Rev. Lett.* **90**, 167002 (2003).

<sup>25</sup>T. Hiejima, S. Yamada, M. Uruichi, and K. Yakushi, *Physica B* **405**, S153 (2010).

<sup>26</sup>T. Kawai and A. Kawamoto, *Phys. Rev. B* **78**, 165119 (2008).

- <sup>27</sup>M. Maesato, Y. Kaga, R. Kondo, and S. Kagoshima, *Phys. Rev. B* **64**, 155104 (2001).
- <sup>28</sup>R. Kondo and M. Maesato, *Kotai Butsuri* **46**, 241 (2011).
- <sup>29</sup>N. Tajima, A. Ebina-Tajima, M. Tamura, Y. Nishio, and K. Kajita, *J. Phys. Soc. Jpn.* **71**, 1832 (2002).
- <sup>30</sup>M. Yamashita, A. Kawamoto, and K. Kumagai, *Synth. Met.* **133-134**, 125 (2003).
- <sup>31</sup>A. Vainrub, S. Vija, E. Lippmaa, V. Prigodin, R. Beha, and M. Mehring, *Phys. Rev. Lett.* **69**, 3116 (1992).
- <sup>32</sup>A. Kawamoto, Y. Honma, and K. Kumagai, *Phys. Rev. B* **70**, 060510 (2004).
- <sup>33</sup>N. Drichko, M. Dressel, C. A. Kuntscher, A. Pashkin, A. Greco, J. Merino, and J. Schlueter, *Phys. Rev. B* **74**, 235121 (2006).